

Interaction of Multiple Cylindrical Expanding Shock Waves



S. Qiu, N. Amen, and V. Eliasson

Abstract The study of shock-shock interaction has interested researchers since the days of Ernst Mach. The nonlinearity of the shocks yields a complex interaction featuring a Mach stem. This phenomenon is very similar to the reflection patterns of a planar shock wave over an inclined wedge. As the shocks expand, the two-shock system is no longer able to turn the flow as much as needed, and a Mach stem is generated. As the shocks continue to expand, so too does the Mach stem. The expansion of a shock wave has been studied analytically by Lin (*J Appl Phys* 25:54–57, 1950) and Taylor (*Proc R Soc Ser A Math Phys Sci* 201:159–174, 1954) for two and three dimensions, respectively. In these cases, however, there is only a single blast. For shock-shock interaction, von Neumann's (*Oblique Reflection of Shocks*. Bureau of Ordnance, Washington, DC, 1943) work using a planar shock wave over a wedge, while similar, does not consider the decaying properties behind an expanding shock wave. This study will focus on two separate numerical methods; geometrical shock dynamics (GSD) and Euler simulations. Each of them was used to study a two-dimensional shock interaction case with two cylindrically expanding shock waves. The results from the GSD and Euler simulations were then compared to analogous experimental work conducted by Higashino et al. (*Shock Waves* 1:275, 1991). Good agreement is seen between the three cases apart from early times in the case of GSD.

S. Qiu

Aerospace and Mechanical Engineering, University of Southern California, Los Angeles, CA, USA

N. Amen · V. Eliasson (✉)

Structural Engineering, University of California, San Diego, La Jolla, CA, USA

e-mail: eliasson@ucsd.edu

1 Introduction

Shock wave focusing is a topic closely related and of interest to both the mathematics and physics communities. Due to the nonlinear nature of shock waves and their interactions with nonuniform or moving media, solid or porous surfaces, or other shock waves, predictions of shock dynamics and shock-focusing events are far from trivial. Our current study aims to deepen the understanding of shock wave focusing processes by studying the interaction of multiple cylindrical interacting shock fronts. The study has been performed using a combination of analytical and numerical tools of which the results were compared to previous experimental work by Higashino et al. [4] in which two cases were studied: the detonation of copper wires and that of Nichrome wires. For the numerical part, cylindrical shock waves were generated in a two-dimensional plane by using suitable initial conditions [2]. During the initial expansion phase, the shocks do not interact with each other. Once they do, the interaction will result in regular reflection that transitions to irregular reflection depending on the strength and the geometry of the shocks. The entire process was simulated by solving the 2D Euler equations of gas dynamics using Overture, a finite-difference solver with overlapping grids and adaptive mesh refinement [5]. Each of the experiment's materials required different initial input energy to detonate, and thus, a different simulation, with corresponding blast energy, was run for each case.

However, to better understand the regular to irregular transition criteria for these types of shock waves, many simulations with different setups could be needed. Because the Euler equations can be time-consuming to solve, a more efficient method was investigated to predict the shock-shock interaction. This was accomplished using GSD where the GSD equations were programmed into a numerical solver and parallelized using a spatial decomposition method coupled with a front-tracking approach [6].

The transition and development of the Mach stem obtained from the Euler simulations and GSD were compared to the ones obtained from the experiment and showed good agreement.

2 Geometrical Shock Dynamics

The use of Euler simulations can be quite computationally expensive. This is because of the need to fully determine the flow field on both sides of the shock front. However, using GSD, proposed by Whitham [7], the computational cost can be reduced significantly. In this method, only the shock front is considered such that the flow conditions in front of and behind the shock need not be computed. The shock front is discretized into many pieces and defined with a velocity normal to the shock segment. In this way, each segment can be visualized as traveling through small ray tubes that may bend themselves in accordance with the area-Mach relation

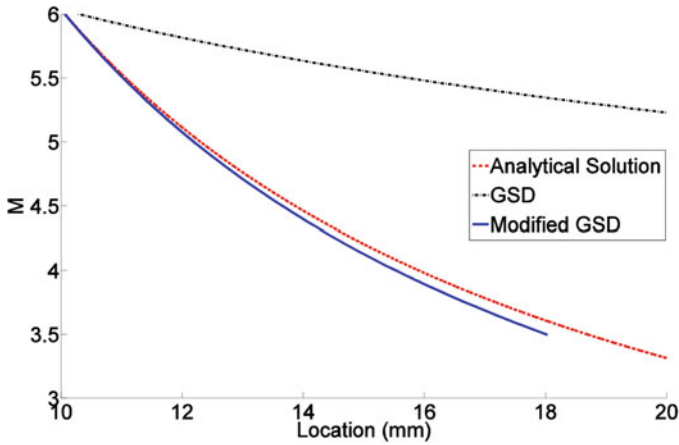


Fig. 1 Cylindrical shock front Mach number versus shock radius

$$\frac{1}{A(x)} \frac{dA}{dM} = -g(M), \tag{1}$$

where

$$g(M) = \frac{M}{M^2 - 1} \left(1 + \frac{2}{\gamma + 1} \frac{1 - \mu^2}{\mu} \right) \left(1 + 2\mu + \frac{1}{M^2} \right), \tag{2}$$

$$\mu^2 = \frac{(\gamma - 1) M^2 + 2}{2\gamma M^2 - (\gamma - 1)} \tag{3}$$

and where γ is the adiabatic index, x is the distance in the ray tube, and the cross-sectional area, $A(x)$, is a function of x . Using GSD, the computational complexity can be reduced by more than an order compared to using Euler equations.

However, Eq. (1) is developed under the assumption that the flow behind the shock is uniform. For cylindrical shocks which expand outward, this assumption is not valid. Comparison between GSD and an analytical solution developed by [8] on a cylindrical shock expanding process has been shown in Fig. 1. The Mach number of the shock front from GSD cannot match the analytical solution, which indicates that the flow behind the shock front is important for the shock expanding process.

2.1 Modified GSD

To better improve the predication of shock expanding process from GSD, the Area-Mach relation has been revisited without taking the original assumption into account.

$$\left(\frac{dp}{dM} + \rho a \frac{du}{dM} \right) \frac{dM}{dt} = - \left[a_0 M \frac{\rho a^2 u}{a+u} \frac{A'}{A} + \left(\frac{a_0 M}{a+u} - 1 \right) \left(\frac{\partial p}{\partial t} + \rho a \frac{\partial u}{\partial t} \right) \right] \quad (4)$$

Equation (4) shows the relation, in which p , a , and u represent pressure, speed of sound, and flow velocity behind the shock, respectively, and a_0 denotes the speed of sound in the ambient air. It should be noted that the last term of Eq. (4) on the right side represents the flow condition behind the shock. Whitham [7] neglected this term because it will be extremely small under the uniform flow assumption. Here, a new approach is proposed to couple the flow conditions behind the shock into Eq. (4), where similitude equations, which are obtained from analytic solutions, experimental data, or other existing numerical data, are developed and implemented into the last term. In addition, a modified GSD scheme based on this approach has been developed. Good agreement between the modified GSD and the analytical solution has been shown in Fig. 1.

3 Euler Simulation Setup

The Euler simulations were run using Overture, which solves partial differential equations using finite-difference methods on overlapping grids with a second-order Godunov scheme [5]. The computational domain was established based on Higashino et al.'s experimental setup that, however, contained only a single expanding shock to take advantage of the line of symmetry along the reflection plane. The computational domain was 105×150 mm with grid size 0.04 mm for both the horizontal and vertical directions. All boundaries are set as a rigid wall with a no slip condition. The center of the cylindrical shock wave is located at $(-30,0)$, which is the same as in the experiment [4]. From the concept of image bursts [9], when the shock hits the wall, it is equivalent to the shock interaction with another shock wave of the same strength at the opposite side of the wall. By using this setup, the computational complexity is reduced to half of the original.

The blast energy was estimated based on the total electrical energy reported by Higashino et al. The blast energy can be calculated as capacitive energy, E_C , calculated as using the capacitance, C , and the voltage, V , expressed as

$$E_C = \text{Explosion energy} = \frac{1}{2} C V^2 \quad (5)$$

and scaled to two-dimensional space using

$$E = \frac{\text{Explosion energy}}{\text{unit line}} (2\pi)^{-1} \quad (6)$$

as defined by [4] to account for the pseudo-two-dimensionality of the experimental work. Using Eq. (5), the computed explosion energies for the copper and Nichrome cases were 25 J and 64 J, respectively. This energy is then used in Eq. (6), where the calculated energy, E , was used in the 2D simulation. The calculated explosion energy for the copper case was close to that of the experiment of 23.12 J; however, a discrepancy was evident for the Nichrome case which was 169.28 J. This is due to the uncertainties derived from the experiment. Because of the finite length of wire used (34 mm), it is likely that the entire wire does not detonate evenly or at all. It is assumed, however, that the entire length is detonated simultaneously. It is also uncertain as to whether the entire capacitive energy was used to facilitate the blast. While this is assumed, it is possible that the wire does not require the full energy and will detonate before the capacitors have been emptied. Because of these uncertainties, the simulation was rerun at an energy of 64 J, which showed better agreement with the experimental results.

4 Result Comparison

The results from the Euler simulations were compared to the experimental work by Higashino et al. [4] and show good quantitative agreement in the results. Table 1 compares the shock arrival times that were quoted by Higashino et al. [4] to the Euler simulations.

Despite the uncertainty in the blast initiation time of the experiment, the arrival times differ by only a maximum of 2 μs for copper wires and by maximum of 4.7 μs in the case of Nichrome wires.

Because of the agreement between Euler simulations and experiments, the GSD results were compared to the Euler results. Figure 2 shows the qualitative comparison of the shock fronts of GSD and Euler simulations via simulated schlieren.

Figure 2 shows the comparison for the copper wire case where the most notable difference between these two is that the Mach stem in the GSD result appears to move faster compared to the Euler simulation result. For the Nichrome wire case, the same results have been found. This is due to the modified GSD code, which, while it takes the decaying properties behind the shock into account during the shock expansion process, it is not able to take advantage of this during the shock-

Table 1 A comparison of shock arrival times of the current Euler simulation versus the experiment presented in [4]

	Higashino et al. [4]	Euler simulation
Copper (a)	83.7 μs	83.8 μs
Copper (b)	181.2 μs	179.2 μs
Nichrome (a)	71.2 μs	66.5 μs
Nichrome (b)	128.7 μs	130.6 μs

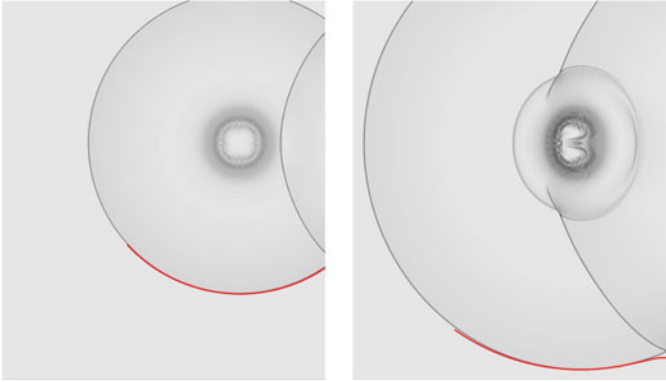
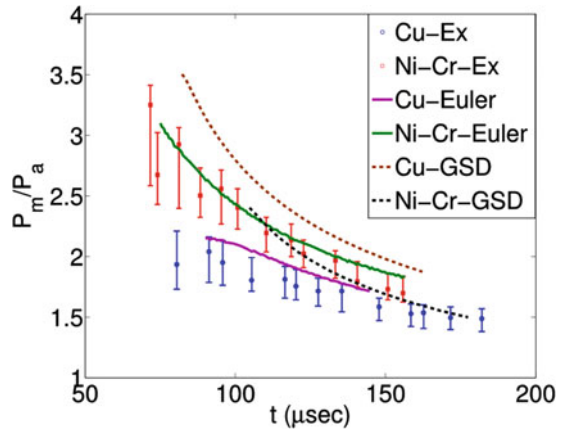


Fig. 2 Overlay of Euler simulation (schlieren background) and GSD (red lines) results for copper wires

Fig. 3 Ratio of maximum pressure P_m , at the Mach stem to ambient pressure P_a , versus time t (experimental data recreated from [4])



shock interaction where the Mach stem is formed. To show this in more detail, the time history of the location of the Mach stem is shown in Fig. 3 for GSD, Euler simulations, and experiments [4].

Here, the dotted brown and black curves correspond to the shock-shock interaction and resulting Mach stem by the GSD, the solid green and purple curves are from Euler simulations, and the red and blue data points are from experiments [4]. For both copper and Nichrome, the Euler curves can be seen to exist almost entirely inside the experimental uncertainty, while both GSD curves overshoot (faster Mach stem) at first and then converge over time to the Euler and experimental results.

5 Conclusion

Euler and geometrical shock dynamics simulations have been performed to match the experiments of Higashino et al. [4]. The results of the simulations showed both good qualitative and quantitative agreement for the detonation of copper wires and Nichrome wires. The GSD showed an overshoot in the Mach stem location compared to both Euler and experiments. This is because the GSD code does not account for the flow properties behind the shock front during the interaction process. Despite the overshoot, the overall accuracy of GSD methods in shock-shock interaction has been shown.

For the future, the GSD code will be modified further to account for the flow properties behind the Mach stem. Once complete, the new GSD code and Euler simulations will be compared to a new exploding wire experiment, in which the uncertainties will be quantified to reduce error. And, with the help of the modified GSD, the Euler simulations, and the experiment, the transition criteria from regular reflection to irregular reflection on shock-shock interaction will be investigated.

References

1. G.I. Taylor, The formation of a blast wave by very intense explosion, I, theoretical discussion. Proc. R. Soc. Ser. A Math. Phys. Sci. **201**, 159–174 (1950)
2. S. Lin, Cylindrical shock waves produced by instantaneous energy release. J. Appl. Phys. **25**(1), 54–57 (1954)
3. J. von Neumann, *Oblique Reflection of Shocks.*, Tech. Rep. No. HDL-TR-1429 (Bureau of Ordinance, Washington, DC, 1943)
4. F. Higashino, L.F. Henderson, F. Shimizu, Experiments on the interaction of a pair of cylindrical weak blast waves in air. Shock Waves **1**(4), 275 (1991)
5. S. Qiu, V. Eliasson, Interaction and coalescence of multiple simultaneous and non-simultaneous blast waves. Shock Waves **26**(3), 287–297 (2016)
6. S. Qiu, K. Liu, V. Eliasson, Parallel implantation of geometrical shock dynamics for two dimensional converging shock waves. Comput. Phys. Commun. **207**, 186–192 (2016). <https://doi.org/10.1016/j.cpc.2016.06.003>
7. G.B. Whitham, *Linear and Nonlinear Waves* (Wiley, Pasadena, 2011)
8. G.G. Bach, J.H.S. Lee, An analytical solution for blast waves. AIAA J. **8**(2), 271–275 (1970)
9. C. Needham, *Blast Waves* (Springer, Albuquerque, 2010)